Available online at www.sciencedirect.com

ScienceDirect

Procedia CIRP 133 (2025) 49–54

www.elsevier.com/locate/procedia

20th CIRP Conference on Modeling of Machining Operations

Simulative approach to investigate the influence of tool deviations on the effective cutting conditions in gear skiving

Emma Punsmann*,[a], Tassilo Arndt[a], Volker Schulze[a]

[a]*wbk Institute of Production Science, Karlsruhe Institute of Technology (KIT), Kaiserstr. 12, 76131 Karlsruhe, Germany*

* Corresponding author. Tel.: +49-1523-9502596 ; *E-mail address:* emma.punsmann@kit.edu

Abstract

In the course of electromobility the demand for resistant and high-precision internal gears is increasing. Gear skiving is a complex manufacturing process offering a good compromise of productivity and flexibility for this application. The process is characterized by a strong variation of the effective cutting conditions across the tool profile and the engagement. Therefore numerical models are required for profound process design. However, common methods for calculating the effective cutting conditions do not take deviations of tool teeth into account.

This work presents a simulative approach to investigate the influence of tool deviations on the effective cutting conditions in gear skiving. An existing penetration calculation is extended to include radial and axial runout and pitch deviation of the tool teeth. An exemplary simulation study is conducted to analyze their influence on the effective cutting parameters with a focus on the detection of extreme values. It is shown that pitch deviations have a significant effect on the uncut chip thickness and the effective rake angle. This effect can be further amplified or mitigated by radial runout deviations.

Keywords: Geometric modelling; Tool geometry; Gear skiving

1. Introduction

Gear skiving is particularly well suited for the production of internal gears and external gears with nearby interfering contours. It represents a balanced trade-off between productivity and flexibility, offering higher productivity compared to gear shaping and greater flexibility compared to broaching. Gear skiving has become increasingly important in recent years which has motivated ongoing research activities and its establishment in series production [1].

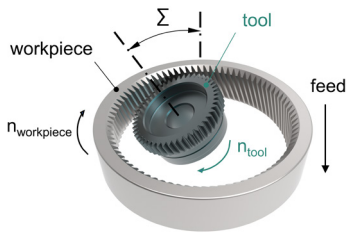

Fig. 1. Schematic view of the skiving process

Characteristic for this process are the synchronously rotating workpiece and tool axes, that are arranged at a axis-crossing angle Σ to each other, creating the cutting speed, see Figure 1. The complex process kinematics lead to a high variance of the effective cutting conditions across the tool profile and engagement [2]. Furthermore the process parameter windows are restricted by negative rake angles and small clearance angles [3].

While early research focused primarily on accurately modeling the skiving process, recent studies increasingly emphasize improving the resulting gear accuracy and quality. With significant advancements in skiving technology and its growing industrial adoption, research now often examines how process-related errors—arising from tool, workpiece, or machine deviations—impact the final gear quality.

Guo et al. introduced a method for calculating the theoretical tooth profile errors of gears machined by skiving with a focus on the influence of the rake angle [4]. Building on the theories of cutter enveloping gear, they analyzed the effects of tool position and orientation errors, as well as tool eccentricity error on skiving accuracy. Their findings revealed a direct relation between tool eccentricity error and profile deviations. Furthermore, the authors investigated the influence of the tooth ratio on

10.1016/j.procir.2025.02.010

helix as well as profile deviations through simulations, thereby highlighting the critical role of tooth cutting order [5].

Lin et al. explored the influence of workpiece pose errors on gear skiving accuracy by mapping the relationship between the skiving tool and the tooth flank of the workpiece. Their analysis demonstrated how workpiece pose errors influence cutting depth and result in tooth deviations [6]. Cousins et al. assessed gear quality after introducing minor alterations to the axis-crossing angle Σ, X-axis shift, and Y-axis shift. Using a Design of Experiments (DoE) approach, they evaluated how cutting tool orientation affects the geometrical characteristics of the finished gear in a series of experiments and developed a statistical model capable of predicting the geometry based on given tool offsets. This model allows tooling errors to be mitigated through positional adjustments within the skiving process [7]. However, their model is constrained by a limited design space, and its findings are only partially generalizable.

In contrast to existing research that primarily focuses on establishing the relationship between skiving parameters and workpiece quality, this work aims to analyze the impact of tool deviations on local effective cutting conditions. Unfavorable cutting conditions, such as negative clearance angles, are expected to not only degrade workpiece quality but also increase tool load and wear. By extending an existing simulation methodology to account for tool deviations, this approach enables the analysis of their effects across various processes. Additionally, the model allows for the transfer of findings to different tool and workpiece geometries, offering a more comprehensive understanding of the interplay between tool deviations and skiving process dynamics.

2. Modeling

The underlying simulation is based on OpenSkiving. OpenSkiving is an open source software for gear skiving kinematics, tool profile, topography and cutting condition calculation developed at the wbk Institute of Production Science [8]. The process kinematics and tool profiles are calculated based on the parameters of profile-shifted conical gears, as presented by Hilligardt and Schulze [9]. This method enables iteration-free process design using predefined gear data for the workpiece and desired tool properties.

The effective local cutting conditions are assessed through a dexel-based geometric penetration calculation on the uncut chip, which was introduced by Hilligardt et al. [10]. In the simulation, the cutting edge is discretized and normal vectors $\vec{N}$, normal rake face vectors $\vec{K}$, normal clearance face vectors $\vec{C}$ and local tangential vectors $\vec{T}$ of the cutting edge are defined for every discrete point. The workpiece is modeled by a number of dexel, with triangulated end points. The uncut chip thickness h is calculated along the cutting edge normal $\vec{K}$ on the rake face for every incremental step. Afterwards the workpiece dexel are trimmed against the triangulated sweep surface of the cutting edge in its current position and the step before. This process is depicted in Figure 2a) and b) in a two-dimensional view.

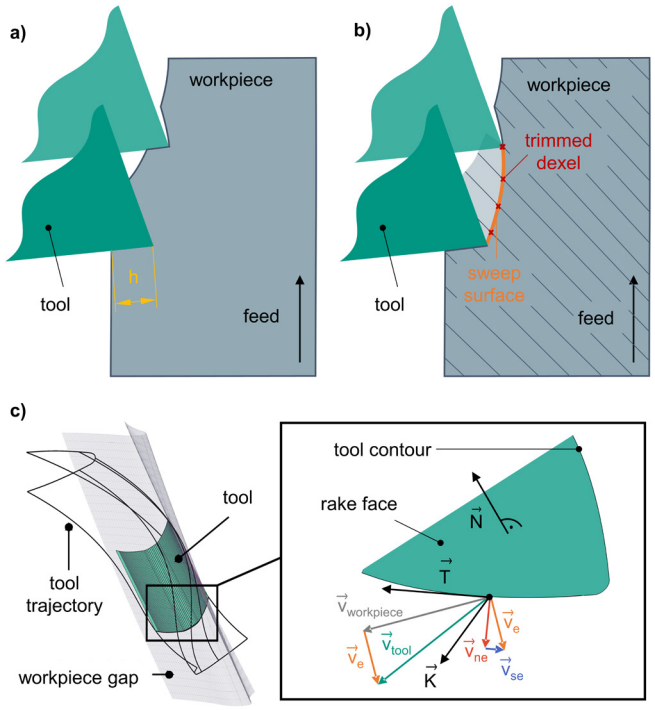

Fig. 2. Illustration of the geometric penetration calculation a) uncut chip thickness calculation b) workpiece trimming c) local normal and speed vectors

The local cutting conditions are derived from the local speed vectors. The resulting effective cutting speed $\vec{v_e}$ corresponds to the relative speed between workpiece and cutting tool and is divided into sliding speed $\vec{v_{se}}$, which is tangential to the cutting edge and the effective normal speed $\vec{v_{ne}}$, see Figure 2c). The effective normal rake and clearance angles, γ_{ne} and α_{ne}, are determined by the relative orientation of the effective normal speed, the local contour normal, and the normal of the clearance face within the cutting edge normal plane [10].

$$\gamma_{ne} = -\arccos\left(\frac{\vec{K}\cdot\vec{v_{ne}}}{\left|\vec{K}\right|\cdot\left|\vec{v_{ne}}\right|}\right)+\frac{\pi}{2} \tag{1}$$

$$\alpha_{ne} = \arccos\left(\frac{\vec{C}\cdot\vec{v_{ne}}}{\left|\vec{C}\right|\cdot\left|\vec{v_{ne}}\right|}\right)-\frac{\pi}{2} \tag{2}$$

The local cutting conditions are calculated for each discrete incremental step and plotted as a function of the tool rotation angle and the x-coordinate along the tool profile. Figure 3a) shows the uncut chip thickness (h) field for the selected process with no consideration of tool deviations. The resulting shape reflects the tool engagement across the leading and trailing flanks, as well as at the tool tip. The color gradient in the plot represents the local uncut chip thickness. The maximum uncut chip thickness occurs at the tool tip shortly after the first contact, while the uncut chip thickness on the leading and trailing flanks remains relatively small and constant.

To facilitate the analysis of multiple processes or cuts, the data is compressed by extracting the extreme values at each point along the tool profile. This is shown in Figure 3b), where the maximum uncut chip thickness at each profile point is highlighted. As observed in part a), the maximum uncut chip thickness occurs at the tool tip.

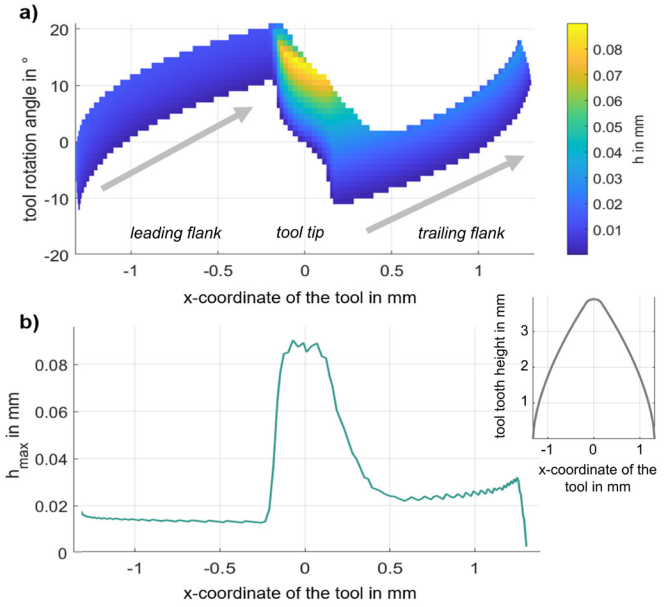

Fig. 3. Effective local uncut chip thickness a) across the tool profile and engagement b) extreme values across the tool profile

2.1. Tool deviations

Skiving tools can be regarded as gears and are typically measured using the same precision measurement systems. Accordingly, the geometric parameters used to assess gear quality also serve as a basis for characterizing tool deviations. DIN ISO 1328-1 specifies the geometric measurements used to determine the quality of spur and helical gears [11]. These parameters are not measured for every tooth. Profile and helix deviations, in particular, are usually assessed through sample measurements on a small selection of representative teeth, whereas the cumulative pitch deviation F_p and total runout deviation F_r are calculated based on measurements across all teeth (Figure 4).

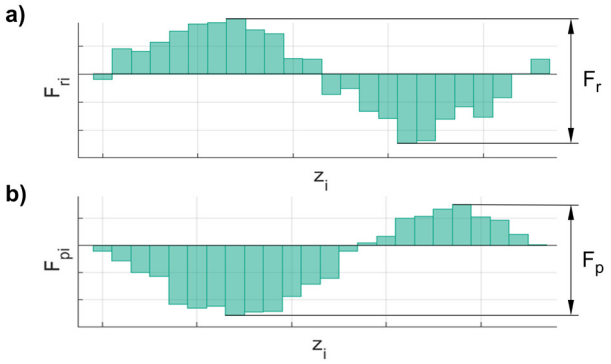

Fig. 4. Definition of F_r and F_p

To streamline the characterization of manufactured tool precision, this modeling approach limits the required input parameters to F_p and F_r. These metrics offer a holistic representation of the tool's actual geometry. Additionally, the setup-related deviations overall radial P_r and axial runout P_p are incorporated into the analysis.

2.2. Transformation of the tool teeth

The ideal geometric profile of the cutting tool tooth is calculated using OpenSkiving, see Figure 6a). The resulting profile is multiplied for each tooth z and subsequently transformed based on the individual deviations calculated from the input parameters. These include the radial deviation F_r, pitch deviation F_p, the setup radial runout P_r and setup axial runout P_p along with the diameter d_{P_p} at which it is measured.

Setup-related deviations (P_r and P_p) are modeled as sinusoidal functions because their measurement methods typically do not provide exact details on the curve's order or progression. Manufacturing deviations (F_r and F_p), on the other hand, are modeled either sinusoidally or linearly based on their respective error orders O_{F_r} and O_{F_p}. As they are typically measured on coordinate measuring machines, the number of orders can be resolved to represent various profiles, accommodating influences such as clamping conditions and tool grinding processes. Three exemplary tool profiles and their corresponding radial deviation orders are illustrated in Figure 5a. To represent the relative positional alignment of the deviation curves, the curves can be shifted by defining a starting tooth z_S, as shown in Figure 5b.

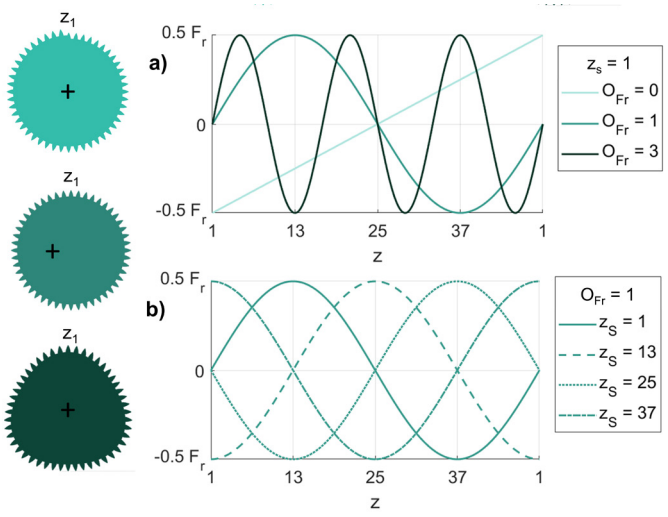

Fig. 5. Modeling of deviation progression a) with different error orders b) with different starting teeth

$$F_r(z_i) = \begin{cases} F_r \cdot \left(-0.5 + \frac{z_i - 1}{z}\right), & O_{F_r} = 1 \\ 0.5 \cdot F_r \cdot \sin\left(O_{F_r} \cdot (z_i - 1) \cdot \frac{360}{z}\right), & O_{F_r} \neq 1 \end{cases} \quad (3)$$

$$P_r(z_i) = 0.5 \cdot P_r \cdot \sin\left((z_i - 1) \cdot \frac{360}{z}\right) \quad (4)$$

The individual radial deviations of each tool tooth z_i are computed in (3) and (4) and applied by translating the tool profile along the Y-axis, see Figure 6b). In homogeneous coordinates this corresponds to (5).

$$T = \begin{bmatrix} 1 & 0 & 0 & 0 \\ 0 & 1 & 0 & F_r(z_i) + P_r(z_i) \\ 0 & 0 & 1 & 0 \\ 0 & 0 & 0 & 1 \end{bmatrix} \tag{5}$$

Pitch deviation (F_p) and axial runout (P_p) are converted to angular deviations ϕ_{F_p} and ϕ_{P_p} relative to the diameter at which they are measured in (6) and (7). These angles are used to transform the tooth profile and associated vectors through rotation matrices (8), ensuring consistency in the altered geometry, see Figure 6c) and d). The transformation is implemented under the assumption that the tooth thickness remains constant.

$$\phi_{F_p}(z_i) = \begin{cases} \frac{2 \cdot F_p}{d} \cdot \left(-0.5 + \frac{z_i - 1}{z}\right), & O_{F_p} = 1 \\ \frac{2 \cdot F_p}{d} \cdot \sin\left(O_{F_p} \cdot (i-1) \cdot \frac{360}{z}\right), & O_{F_r} \neq 1 \end{cases} \tag{6}$$

$$\phi_{P_p}(z_i) = \arcsin\left(\frac{P_p}{d_{P_p}}\right) \cdot \sin\left((z_i - 1) \cdot \frac{360}{z}\right) \tag{7}$$

$$R = \begin{bmatrix} 1 & 0 & 0 & 0 \\ 0 & \cos(\phi_{P_P}) & -\sin(\phi_{P_P}) & 0 \\ 0 & \sin(\phi_{P_P}) & \cos(\phi_{P_P}) & 0 \\ 0 & 0 & 0 & 1 \end{bmatrix} \cdot \begin{bmatrix} \cos(\phi_{F_P}) & -\sin(\phi_{F_P}) & 0 & 0 \\ \sin(\phi_{F_P}) & \cos(\phi_{F_P}) & 0 & 0 \\ 0 & 0 & 1 & 0 \\ 0 & 0 & 0 & 1 \end{bmatrix} \tag{8}$$

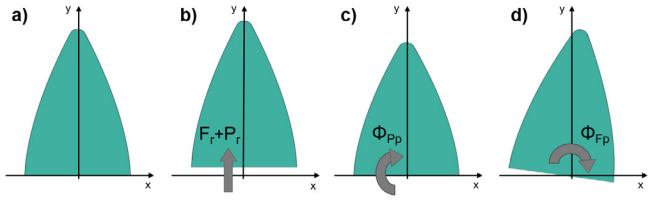

Fig. 6. a) ideal tool profile b) tool profile with radial deviation c) tool profile with axial deviation d) tool profile with pitch deviation

3. Simulation study

The influence of the chosen tool deviations on the local cutting conditions is investigated in an exemplary simulation study. This study is designed to serve as a qualitative example, aiming to provide an initial assessment of the effects on the local cutting conditions. To maintain focus the workpiece geometry, the tool geometry and the process kinematics were fixed, see (Table 1). The selection of these parameters aligns with experiments conducted in a previous study at wbk Institute of Production Science, enabling comparison in subsequent validation experiments.

Table 1. Workpiece, tool and process data

Workpiece data		
Number of teeth	z_2	-82
Normal module	m_n	1.34 mm
Normal pressure angle	α_n	17.5°
Helix angle	β_2	22.5424°
Tip diameter	d_{a2}	115.5 mm
Root diameter	d_f	123.08 mm
Generating addendum modification coefficient	x_e	0.1655
Tooth width	b_2	25 mm
Tool and process data		
Number of teeth	z_0	48
Tip diameter	d_{a0}	69.09 mm
Constructive tip clearance angle	α_c	0°
Helix angle	β_0	0°
Constructive tip rake angle	γ_c	0°
Stair angle	τ	0°
Axis-crossing angle	Σ	24.75°
Immersion depth	T	0.3 mm
Rotational speed	n_0	1290 rev/min
Feed rate	f	0.3 mm/rev

Variable parameters encompassed are the kinds and values of tool deviations and their progression. Individual deviations as well as selected combinations are analyzed to capture potential interactions and their effects on the machining process. The values of the parameters can be seen in Table 2.

Table 2. Factors of the simulation study

single deviation		
deviation	F_r; F_p; P_r; P_p	
value	0.01; 0.05	P_p measured at $d_{P_p} = 60mm$
error order	0; 1; 3	only varied for F_r and F_p
double deviations		
deviation	F_r; F_p; P_r; P_p	
value	0.01; 0.05	P_p measured at $d_{P_p} = 60mm$
error order	0; 1	only varied for F_r and F_p
starting tooth	1; 13; 25; 37	

For each simulation the effective local cutting conditions across all tool profiles are calculated and the influence of the tool deviations is analyzed based on the extreme values along the cutting trajectory.

4. Results and discussion

The simulation enables the assessment of local cutting conditions for each individual tool tooth. To illustrate the insights that can be gained from the simulation study a few exemplary results are presented with a particular focus on the effects of pitch deviations on local uncut chip thickness.

Simulations were conducted using a realistic tool deviation of 0.01 mm [11] and an exaggerated deviation (increased by a factor of five), see Table 2. This amplification was introduced to enhance the visibility of the tool deviations' impact on the characteristic maps and extreme values. As the exact outcomes are highly dependent on specific use cases, the main goal here

is to provide a qualitative assessment; thus, most of the results employ the deviation value of 0.05 mm. However, exemplary results of the investigated process with deviations of 0.01 mm are also provided in Figure 9 for reference.

The deviations within a single cut depend on the relative deviation between the current and the preceding tool tooth. Figure 7 displays the transverse section of the workpiece gap alongside the corresponding characteristic map of the uncut chip thickness for three tool engagement scenarios: negative relative pitch deviation, no (relative) pitch deviation and positive relative pitch deviation. The deviations have an apparent effect on the shape of the characteristic map, leading to pronounced asymmetric loading on the two cutting edges.

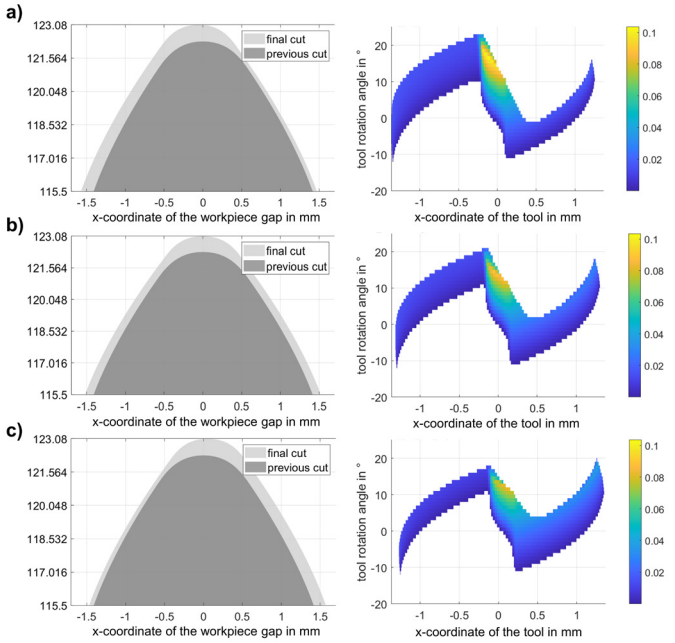

Fig. 7. Transverse section of the workpiece gap and characteristic map of the uncut chip thickness with a) negative relative pitch deviation b) no (relative) pitch deviation c) positive relative pitch deviation

The depicted scenarios arise from a sinusoidal pitch deviation pattern (as shown in Figure 8a)) and the given tooth count ratio. For tooth z_i, the preceding cutting tooth is z_{i-34}, resulting in relative pitch deviation $F_{p,rel\,i}$. The maximum relative pitch deviation of $0.8F_p$ occurs for tooth z_{18} and the minimum relative pitch deviation for z_{42}, see Figure 8b).

Figure 8c) displays the maximum uncut chip thickness across the tool profile for the three engagement scenarios, which, as noted earlier, can occur on different teeth within the same tool. The results show that tool teeth with positive pitch deviation experience increased maximum uncut chip thickness at the tip and reduced thickness on the leading flank compared to the ideal process or teeth with no relative pitch deviation. This shift results in a higher load concentrated at the tool's tip. Conversely, for teeth with negative relative pitch deviation, the maximum uncut chip thickness is more evenly distributed across the profile. Additionally, this effect significantly influences the progression of the minimum rake angle, as shown in Figure 8d).

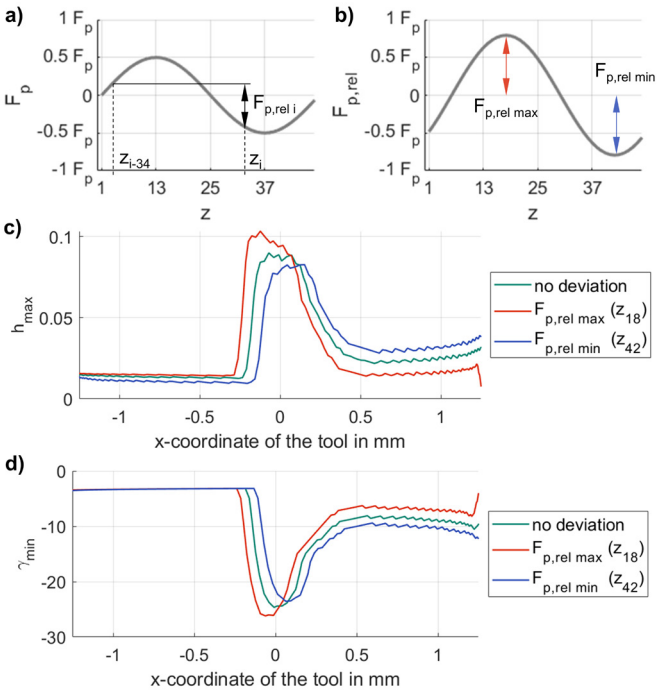

Fig. 8. a) Progression of the pitch deviation b) Resulting relative pitch deviation c) Maximum uncut chip thickness and d) Minimum rake angle

Figure 9c) presents the results of an identical analysis with a realistic pitch deviation of 0.01 mm, enabling a quantitative assessment of its effect on the maximum uncut chip thickness for the selected process. The progression of the maximum uncut chip thickness curves across the tool are similar to those in Figure 8c), albeit less pronounced. For an easily comprehensible yet informative assessment, the values are combined and presented as a boxplot for the tool tip, leading and trailing flank.

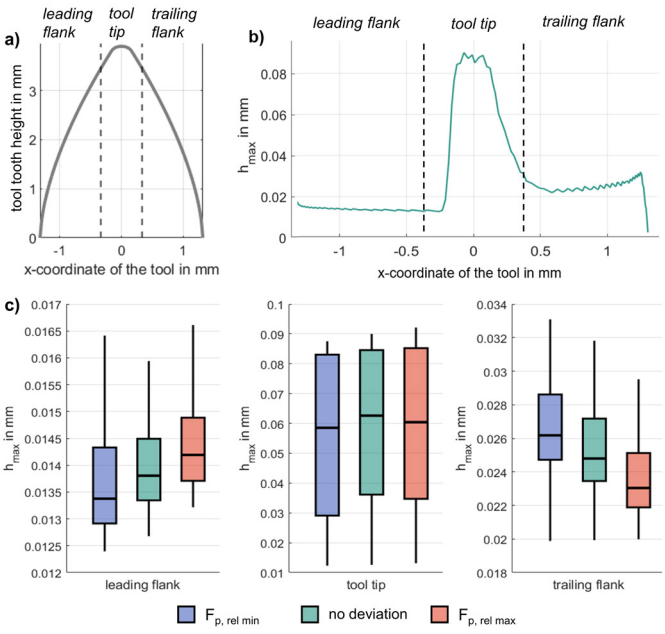

Fig. 9. a) Definition of leading flank, tool tip and trailing flank across the tool profile b) Division of the maximum uncut chip thickness curve c) Boxplot of the maximum uncut chip thickness for $F_p = 0.01mm$

The chosen definition of the leading flank, tool tip, and trailing flank is illustrated in Figure 9a) over the tool profile and in Figure 9b) on the characteristic curve of the maximum uncut chip thickness. Although the transition between these regions is continuous, for the purpose of dividing the values into three distinct plots the upper 10% of the tool tooth height is defined as the tool tip, while the remaining regions are classified as the leading and trailing flanks, respectively. Based on this definition, two boundaries in the tool's x-coordinate were determined.

Combinations of tool deviations were also analyzed, with particular focus placed on the combination of F_p and F_r. The impact of P_p was found to be relatively minor in comparison, and P_r exhibited behavior similar to F_r. When P_r and F_r act in opposite directions, their effects can cancel each other out, but they more commonly overlap and combine their influences. Figure 10 illustrates the superposition of the previously discussed pitch deviation with a sinusoidal runout deviation, each with a magnitude of 0.05 mm. In one case, the two deviations align identically, while in the other, the starting tooth is shifted to create a 180° phase shift, resulting in an opposite progression of the deviations.

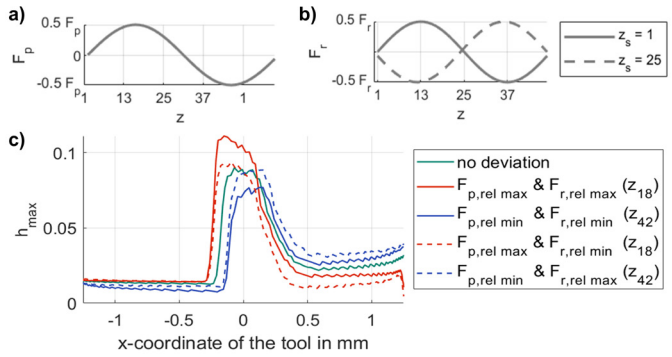

Fig. 10. a) Progression of the pitch deviation b) Progression of the radial runout c) Maximum uncut chip thickness of the extrema of the combined deviations

Figure 10c) displays the maximum uncut chip thickness for the extrema of the combined deviations. When F_p and F_r align identically, the effect described in Figure 8 is further amplified. Conversely, when they have opposite progressions, the uncut chip thickness approaches the reference process. A comparison of these results with the effects of individual deviations reveals that their interaction can even mitigate the overall impact on the uncut chip thickness.

5. Conclusion

This work introduced a simulative approach to investigate the influence of tool deviations on the effective cutting parameters in gear skiving. An existing penetration calculation was extended to account for radial and axial runout as well as pitch deviation of tool teeth and a simulation study was conducted for an example process to qualitatively assess their effects on effective cutting parameters. The analysis highlighted the importance of accounting for both manufacturing-related and setup-related tool deviations to accurately simulate the effective process parameters. It is demonstrated that cutting conditions are strongly influenced by the alignment of deviations from the preceding tool tooth within the workpiece gap and by the interplay of different tool deviations. This works enables more precise simulation results and lays the foundation for establishing a relationship between the effective cutting conditions and machining performance factors, such as workpiece quality and tool wear. Future research will focus on investigating the effect of the uncut chip thickness on burr formation in gear skiving.

Acknowledgments

The authors wish to thank the Deutsche Forschungsgemeinschaft (DFG, German Research Foundation) for funding the project 'Method for minimizing flank burrs in gear manufacturing on the example of gear skiving' – 515118675.

References

[1] Hilligardt, A., Klose, J., Gerstenmeyer, M., Schulze, V. (2022), Modelling and prevention of meshing interference in gear skiving of internal gears, Forschung im Ingenieurwesen, vol. 48, pp. 673–681.
[2] Vargas, B., Zapf, M., Klose, J., Zanger, F., Schulze, V. (2019), Numerical Modelling of Cutting Forces in Gear Skiving, Procedia CIRP, vol. 82, pp. 455–460.
[3] Bauer, R. (2018), Modellbasierte Auslegung von Mehrschnittstrategien beim Wälzschälen, Dissertation, Technical University Chemnitz.
[4] Guo, Z., Mao, S., Li, X., Ren, Z. (2017), Research on the theoretical tooth profile errors of gears machined by skiving, Mechanism and Machine Theory, vol. 97, pp. 1-11.
[5] Guo, Z., Mao, S., Du, X., Ren, Z. (2017), Influences of tool setting errors on gear skiving accuracy, The International Journal of Advanced Manufacturing Technology, vol. 91, pp. 3135-3143.
[6] Lin, X., Hong, R., Wang, Y., Peng, Y., Ren, X., (2022), Influences of the workpiece pose errors on gear skiving accuracy, The International Journal of Advanced Manufacturing Technology, vol. 120, pp. 361–376.
[7] Cousins, B., Curtis, D., Farmery, M., Cook, B. (2024), Power-skiving tool offsets and the feasibility of using a calculator for manipulating the resulting geometry, GEARSolutions, https://gearsolutions.com/features/power-skiving-tool-offsets-and-the-feasibility-of-using-a-calculator-for-manipulating-the-resulting-geometry/, accessed 18 November 2024.
[8] Hilligardt, A., Klose, J., Schulze, V., OpenSkiving [Software], version 2.0, https://openskiving.kit-campus-transfer.de/, accessed 18 November 2024.
[9] Hilligardt, Schulze, V. (2022), A holistic approach for gear skiving design enabling tool load homogenization, CIRP Annals, vol. 71, pp. 85–88.
[10] Hilligardt, A., Böhland, F., Klose, J., Gerstenmeyer, M., Schulze, V. (2021), A new approach for local cutting force modeling enabling the transfer between different milling conditions and tool geometries, Procedia CIRP, vol. 102, pp. 138–143.
[11] Deutsches Institut für Normung (2013), DIN ISO-1328-1: Definitionen und zulässige Werte für Abweichungen an Zahnflanken.